International Journal of Geosynthetics and Ground Engineering (2021) 7:11
https://doi.org/10.1007/s40891-021-00255-0

ORIGINAL PAPER

Performance of Microfine Cement Grouted Sands Under Quick Loading Conditions

Ioannis A. Pantazopoulos[1] · Ioannis N. Markou[2] · Dimitrios K. Atmatzidis[1]

Received: 10 November 2020 / Accepted: 17 January 2021 / Published online: 5 February 2021

Abstract

An experimental investigation was conducted to evaluate the influence of factors pertinent to the suspension and the sand on the effectiveness of microfine cement grouts under quick loading conditions, that is, conditions, where the grouted soil mass is loaded at a rate which is much faster than the rate of pore water pressure dissipation and total stress behavior may be of interest. Unconfined compression and unconsolidated-undrained triaxial compression tests were conducted on grouted sand specimens obtained by injecting suspensions of 12 cements with three water to cement (W/C) ratios into four sands with different grain sizes. A Mohr–Coulomb type linear failure criterion describes satisfactorily the shear strength behavior of cement grouted sands in total stress terms. The values of the activated shear strength parameters generally increase with increasing axial deformation during loading. Grouting with suspensions having W/C = 1 yields unconfined compression strength of grouted sands up to 9 MPa, adds cohesion to the sands reaching 1.7 MPa, increases by 6–14 times the initial modulus of elasticity, reduces by 5–10 times the failure deformation and may increase up to 20% the angle of internal friction of the sands. The stress–strain–strength behavior of sands grouted with suspensions having W/C = 1 is similar to that of cement suspension sediments with the same W/C ratio, whereas the behavior of sands grouted with suspensions having W/C = 3 is similar to that of the clean sands.

Keywords Microfine cement grouting · Limestone sands · Unconfined compression · Unconsolidated-undrained triaxial compression · Deformability · Shear strength

Introduction

Originally developed in Japan in the 1970s and introduced to the USA in the 1980s, microfine cement was intended to be an alternative to chemical solution grouts by extending the application range of ordinary cement grouts in permeation grouting for ground improvement and, as a result, to reduce the use of harmful chemical solutions. Microfine cement is commonly an extremely fine-ground Portland cement that is often mixed with varying amounts of blast furnace slag or pumice [1]. Although the cost of microfine cement is typically five to ten times higher than ordinary Portland cement [1], this higher cost is often more than offset by the advantages and overall superior performance of microfine cement grouts. For that reason, microfine cement products are now widely available around the world and the worldwide use of microfine cement grouts has grown substantially in the last two decades. A variety of projects utilizing different microfine cement grouts has been reported by Henn and Soule [1]. Quantification of the static mechanical properties of the grouted mass for the design of structural grouting projects is mostly based on unconfined compression test results, although it is generally accepted that this test type is primarily utilized as "index test" in parametric and comparative analyses of the grouted soil strength and that the triaxial compression test best simulates field conditions and provides the required design parameters. Consequently, the

✉ Ioannis N. Markou
imarkou@civil.duth.gr

Ioannis A. Pantazopoulos
pantazo@upatras.gr

Dimitrios K. Atmatzidis
dka@upatras.gr

[1] Department of Civil Engineering, Geotechnical Engineering Laboratory, University of Patras, 26504 Patras, Greece

[2] Department of Civil Engineering, Soil Mechanics and Foundation Engineering Laboratory, Democritus University of Thrace, University Campus-Kimmeria, 67100 Xanthi, Greece

documentation of the effectiveness of microfine cements for permeation grouting and the effects of various factors on grouted sand behavior have been the objectives of several research efforts based on unconfined compression testing [e.g., 2–16]. Additional, relatively limited in number, laboratory investigations of the mechanical behavior of sands grouted with ordinary and microfine cement suspensions include results obtained from consolidated-drained [8, 17–21], consolidated-undrained [17, 22–25] and unconsolidated-undrained [26, 27] triaxial compression tests. Direct shear tests have also been conducted on microfine cement grouted sand specimens to quantify the shear strength parameters of grouted sands [28].

The experimental investigation reported herein is part of an extensive research effort aimed toward the development of a relatively fine-grained material, suitable for permeation grouting, obtained by pulverizing ordinary cements produced in Greece. Suspensions of three different cement types, each at four different gradations, were available. It is emphasized that the cements tested are new materials, covering the range from ordinary to microfine cements, for which the anticipated performance was documented in terms of groutability and effectiveness under different loading conditions. The experimental investigation and modeling of suspension groutability and the dynamic properties of grouted sands have been presented elsewhere [29–32]. The effectiveness of these new cement grouts, in terms of strength and deformability of the grouted sands under quick monotonic loading conditions, is the objective of the study reported herein. It should be noted that "quick loading" conditions refer to field situations (such as, excavation of a tunnel or an open pit in or adjacent to the grouted soil mass), where the grouted soil mass is loaded at a rate which is much faster than the rate of pore water pressure dissipation and total stress behavior may be of interest. Although unconfined compression tests have been extensively used in the past for quantifying the strength of microfine cement grouted sands, they were utilized as "index tests" in this investigation to expedite the initial parametric and comparative analysis required for every new grouting material. The main part of this investigation is based on unconsolidated-undrained (UU) triaxial compression tests which serve to enrich and supplement the relatively limited available information on the behavior of microfine cement grouted sands under quick loading conditions. Accordingly, this presentation includes: (a) quantification of the improvement of the strength and deformability of sands by grouting with coarse- and fine-grained cements, (b) documentation of the effect of cement type and fineness, grout composition (water to cement ratio, superplasticizer addition) and sand characteristics (grain size, relative density, degree of saturation prior to grouting) on the effectiveness of these cement grouts, (c) comparison of the grouted sand properties with those of the neat grout and the clean sands and, (d) evaluation of the development of shear strength parameters with axial deformation. The unconfined compression tests and the UU triaxial compression tests required for the present investigation were conducted on grouted sand specimens produced using a specially constructed grouting apparatus. Similar tests were also conducted for the determination of the strength and deformation characteristics of neat cement grouts and clean sands.

Materials and Experimental Procedures

For the purposes of this investigation, three ordinary cement types (Portland, Portland-composite and pozzolanic cement, code-named CEM I, CEM II/B-M and CEM IV/B, respectively, according to the European Standard EN 197-1 [33]) were used. These cements are referred hereafter as CEM I, CEM II and CEM IV. Each ordinary cement was pulverized, by dry grinding in a special laboratory mill, to produce three additional cements with nominal maximum grain sizes (d_{max}) of 40 μm, 20 μm and 10 μm. The gradation characteristics shown in Table 1 indicate that all cements with nominal $d_{max} = 10$ μm can be considered as "microfine", since they satisfy the requirements of European Standard EN 12715 ($d_{95} < 20$ μm and specific surface over 800 m^2/kg [34]) as well as definitions adopted by the American Concrete Institute (ACI) Committee 552, the International Society for Rock Mechanics (ISRM) and the Portland Cement Association (PCA) [1]. Cements with nominal $d_{max} = 20$ μm have adequately small characteristic grain sizes to be considered, marginally, as "microfine".

Table 1 Gradation characteristics of cements

Grain sizes Specific surface	Cement type											
	CEM I				CEM II				CEM IV			
d_{max} (μm)[a]	100	40	20	10	100	40	20	10	100	40	20	10
d_{95} (μm)	57.0	22.5	11.5	8.2	45.5	25.8	13.6	9.1	48.0	26.0	12.8	9.8
d_{50} (μm)	16.6	8.6	4.2	3.2	14.0	9.4	5.8	4.2	14.2	9.3	4.4	3.9
d_{10} (μm)	3.0	2.0	1.2	1.0	2.2	2.0	1.4	1.1	3.0	2.2	1.3	1.2
Blaine (m^2/kg)	384	529	710	920	466	591	735	942	452	582	715	923

[a]Nominal maximum cement grain size

All suspensions tested during this investigation were prepared using potable water, since it is considered appropriate for preparing cement-based suspension grouts [35, 36]. The water to cement (W/C) ratio of the suspensions was set equal to 1, 2 and 3 by weight, because suspensions with a W/C ratio higher than 3 would have prohibitively large bleeding, long setting times and low strengths, whereas suspensions with a W/C ratio lower than 1 would have prohibitively high viscosity [27, 35, 37, 38]. A superplasticizer based on polycarboxylate chemistry was used to improve the suspension properties of all cements. For comparison purposes, unconfined compression and UU triaxial compression tests were conducted on specimens of selected grouts with W/C ratio equal to 1 (stable suspensions) after curing for 28 days. The curing and testing conditions were identical to those used for grouted sands and the results obtained are presented in Table 2.

The soils used were clean and uniform limestone sands with angular grains. Four different sands were used with grain sizes limited between ASTM sieve sizes [40] Nos. 5–10, 10–14, 14–25 and 25–50 having the gradation characteristics given in Table 3. The shear strength and deformability parameters summarized in Table 3 were obtained by conducting UU triaxial compression tests on sand specimens, in dry and dense condition, under confining pressures equal to 100, 200 and 400 kPa.

The laboratory equipment shown in Fig. 1 was designed according to ASTM Standard D4320-02 [41] and used for the production of grouted sand specimens, with a height of 112 mm and a diameter of 50 mm, ready for testing without cutting or trimming. The grout tank and split molds were made of plexiglass to allow visual checking of the injection process. The sands were placed in the molds at a dry and dense state (relative density ranging from 90 to 95%). All suspensions were prepared using two high-speed mixers of the type used for the preparation of soil specimens for hydrometer testing, with a speed of 10,000 rpm at no load. As recommended by the superplasticizer producer, the appropriate amount of cement and 70% of the required water were placed in the mixer together with the superplasticizer dosage and mixed for 5 min. Then, the rest of the water was added and mixing continued for another 5 min. The superplasticizer dosage was set equal to 1.4% by weight of dry cement for all suspensions after an experimental documentation of the effect of various dosages on the apparent viscosity and rheological characteristics of the pulverized cement suspensions [39]. Suspensions were injected at the lowest possible pressure until the volume of the injected grout was equal to two void volumes of the sand in each mold. 24 h after injection, the grouted specimens were extracted from the split molds, placed in plastic film, sealed in plastic bags and immersed in water of constant temperature (≈ 20 °C)

Table 2 Strength and deformability of selected cement grouts (W/C = 1)

Cement		Unconfined compression tests		Unconsolidated—undrained triaxial compression tests			
Type	d_{max} (μm)	Strength q_u (MPa)	Failure deformation ε_f (%)	Initial modulus of elasticity E_i (MPa)	Failure deformation ε_f (%)	Cohesion c (kPa)	Angle of internal friction φ (°)
CEM II	40	12.7	0.7	24.4–37.3	0.5–1.2	840	61
CEM II	20	10.6	0.7	20.6–25.0	0.4–1.1	790	59
CEM II	10	9.7	0.9	21.3–24.3	0.6–1.0	710	58
CEM I	20	6.5	0.8	21.5–28.9	0.7–1.0	1040	61
CEM IV	20	7.0	0.6	17.9–23.7	0.7–1.2	1700	53
CEM IV	10	6.6	0.4	22.1–29.0	0.5–0.9	560	61

Table 3 Gradation characteristics, strength and deformability of sands

Sand	Grain size limits (mm)	Effective grain diameter d_{10} (mm)	Uniformity coefficient C_u	Unconsolidated – undrained triaxial compression tests			
				Relative density D_r (%)	Initial modulus of elasticity E_i (MPa)	Failure deformation ε_f (%)	Angle of internal friction φ (°)
5–10	4.00–2.00	2.15	1.40	97	1.5–2.3	6.2–11.4	40.3
10–14	2.00–1.40	1.45	1.19	99	1.6–2.4	5.8–9.6	42.2
14–25	1.40–0.71	0.77	1.43	94	1.5–2.5	5.7–9.3	42.6
25–50	0.71–0.30	0.34	1.56	92	1.7–2.3	5.3–10.1	42.6

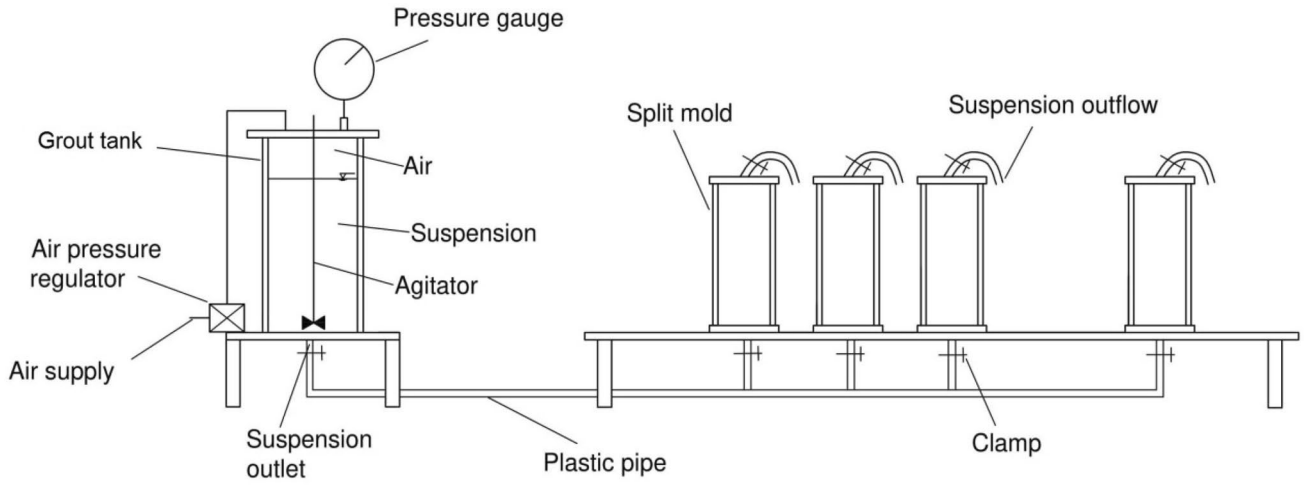

Fig. 1 Equipment for grouting sand specimens

for curing. The grouted sand specimens were tested at their "as-produced" water content, after a total curing period of 28 days, in unconfined compression at an axial strain rate equal to 0.1 mm/min and in UU triaxial compression, at the same axial strain rate, under confining pressures of 100, 200 and 400 kPa.

The combination of 36 suspensions (3 cement types at 4 gradations and 3 W/C ratios) and 4 sand gradations incorporated in the present research yields an excessive number of combinations for conducting unconfined compression and triaxial compression tests. Therefore, the laboratory investigation is centered on the 12 suspensions of CEM II cement injected into dry and dense 14–25 sand. The choice of CEM II cement was based on (a) the observation that its suspensions exhibited the best overall behavior compared to suspensions of the other two cement types [39], (b) the relative ease of grinding for the production of microfine cements, (c) the observation that similar cement types have been studied on a smaller scale in the past, and (d) the fact that its industrial production is more economical and less energy-intensive compared to CEM I cement. The 14–25 sand was chosen, because it is the finest sand in which the thickest cement grouts (W/C = 1) could be easily injected. The testing program was supplemented with selected suspension—sand combinations to investigate the effect of parameters such as superplasticizer addition and sand characteristics.

Unconfined Compression Tests

Typical stress–strain curves obtained from unconfined compression tests conducted on grouted sand specimens are presented in Fig. 2 together with the stress–strain curve obtained for a neat grout specimen prepared with the same cement and W/C = 1. In general, the stress–strain curves of the grouted sand specimens tested have similar forms consisting of an initial linear or nearly linear part followed by an extended plastic area about failure (maximum value of axial stress). The plastic failure zone is usually less pronounced in sands grouted with suspensions having W/C = 1 due to stronger cementation. This argument is supported by the typical stress–strain curve of grout shown in Fig. 2, which resembles those of grouted sands in the initial part but exhibits a more brittle failure form than the grouted sands. The unconfined compression strength of neat grouts having W/C = 1 (Table 2), compared to that of sands grouted with the same suspensions, depends on cement type, since it is approximately equal for CEM I cements, higher for CEM II cements (Fig. 2) and lower for CEM IV cements.

The unconfined compression strength of all grouted sands tested ranges generally from 0.5 to 9.1 MPa. The results obtained indicate that the suspension W/C ratio has a strong effect on the unconfined compression strength of the grouted sands. As shown in Fig. 3a, grouting with thick cement suspensions (W/C = 1) resulted in strength values ranging from 4 to 9.1 MPa. Sands grouted with the thinner suspensions, having W/C ratio equal to 2 and 3, obtained strength values ranging from 0.5 to 2.4 MPa and from 0.5 to 1 MPa, respectively. This substantial strength increase with decreasing suspension W/C ratio has also been observed by several other researchers [e.g., 2–4, 6, 8, 9, 13, 15, 16, 42, 43] for sands grouted with ordinary and microfine cement suspensions and can be attributed (a) to the increase of the unconfined compression strength of the grout sediments with decreasing suspension W/C ratio from 2 and 3 to 1 [39] and (b) to the more effective filling of sand voids with grout solids [4] caused by the decreased suspension bleed capacity as the W/C ratio decreases. The failure deformation, ε_f,

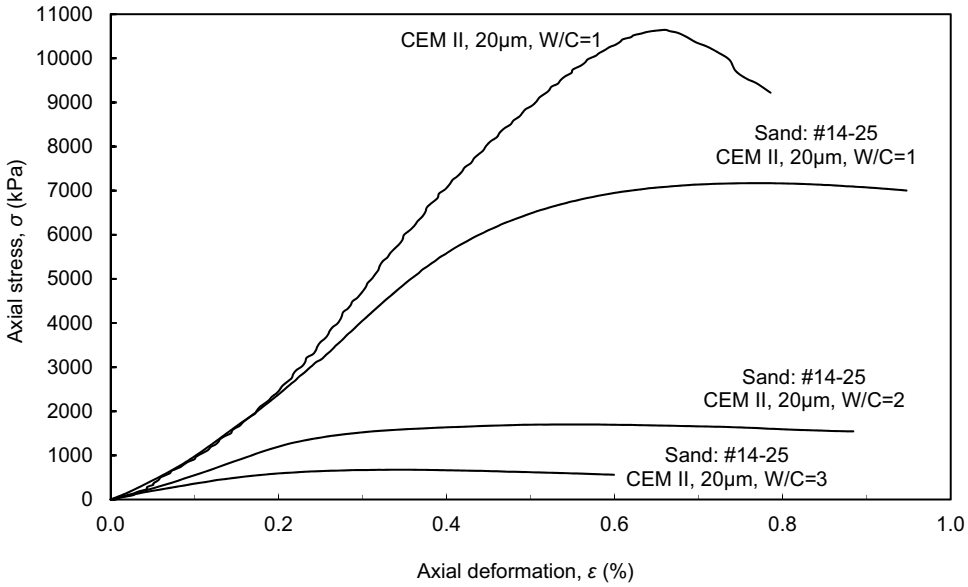

Fig. 2 Stress–strain curves of cement grout and grouted sand from unconfined compression tests

(axial deformation corresponding to the maximum value of axial compression stress) of all grouted sands tested ranges between 0.27 and 1.10% and, as shown in Fig. 3b, decreases with increasing suspension W/C ratio. The failure deformations of neat grout specimens obtained from suspensions having W/C ratio equal to 1 and sands grouted with the same suspensions are comparable, as they range from 0.4 to 0.9% (Table 2) and from 0.45 to 1.10% (Fig. 3b), respectively.

It has been shown [3, 44] that use of microfine cements can lead to higher unconfined compression strength values of grouted soil in comparison to grouting with ordinary Portland cements. This effect is verified by the data presented in Fig. 3c. It can be observed that the unconfined compression strength of the grouted sands increases with decreasing cement grain size, especially for thick grouts (W/C = 1). This behavior has been attributed to the observed increase of the unconfined compression strength of neat cement sediments with similar sediment W/C ratios caused by the increase of cement fineness, mainly due to the higher hydration activity of finer grains and more efficient hydration process [39]. However, the effect of cement grain size on the unconfined compression strength of grouted sands is reduced or becomes negligible for suspensions with W/C ratio equal to 2 and 3, respectively. Also, as shown in Fig. 3d, the failure deformation of grouted sands is not consistently affected by cement grain size.

All tests reported herein were conducted on sand samples grouted with suspensions containing superplasticizer at a dosage of 1.4% by weight of dry cement. The use of superplasticizers is a common practice in field applications for improving the rheological behavior of, mostly microfine, cement suspensions. Accordingly, a limited investigation of superplasticizer effect was conducted based on testing of 10–14 sand grouted with suspensions of the three ordinary cements ($d_{max} = 100$ μm) having W/C = 1. The unconfined compression strength values obtained range from 4 to 4.2 MPa and from 5.3 to 5.9 MPa for suspensions with and without superplasticizer, respectively. The limited amount of data not withstanding, it is observed that the addition of superplasticizer to the suspensions caused a reduction of the grouted sand strength by an average of about 25%. This finding is in reasonable agreement with reported slight strength reduction as a result of superplasticizer presence [10] and in disagreement with the strength increase caused by superplasticizer addition [6, 45], probably due to material and/or dosage differences.

The effect of cement type on the unconfined compression strength of grouted sand was investigated by grouting 14–25 sand with suspensions of 9 cements (3 cement types at 3 gradations) having W/C = 1, and the results obtained are presented in Fig. 3e. A systematic effect of cement type is not observed as CEM I yields the highest strength values when grouting with cements having d_{max} equal to 100 μm and 40 μm and CEM IV yields the highest strength value when grouting with cements having d_{max} equal to 20 μm.

The effect of sand grain size on the unconfined compression strength of grouted sand was evaluated by injecting all four available sand gradations (5–10, 10–14, 14–25 and 25–50) with CEM II cement suspensions having $d_{max} = 10$ μm and W/C = 2 as well as two sand gradations (10–14 and 14–25) with CEM I and CEM IV cement suspensions having $d_{max} = 100$ μm and W/C = 1. The results obtained are presented in Fig. 3f and indicate that the strength of grouted sands increases with increasing sand fineness (decreasing effective sand grain size). This influence of sand grain size on the unconfined compression

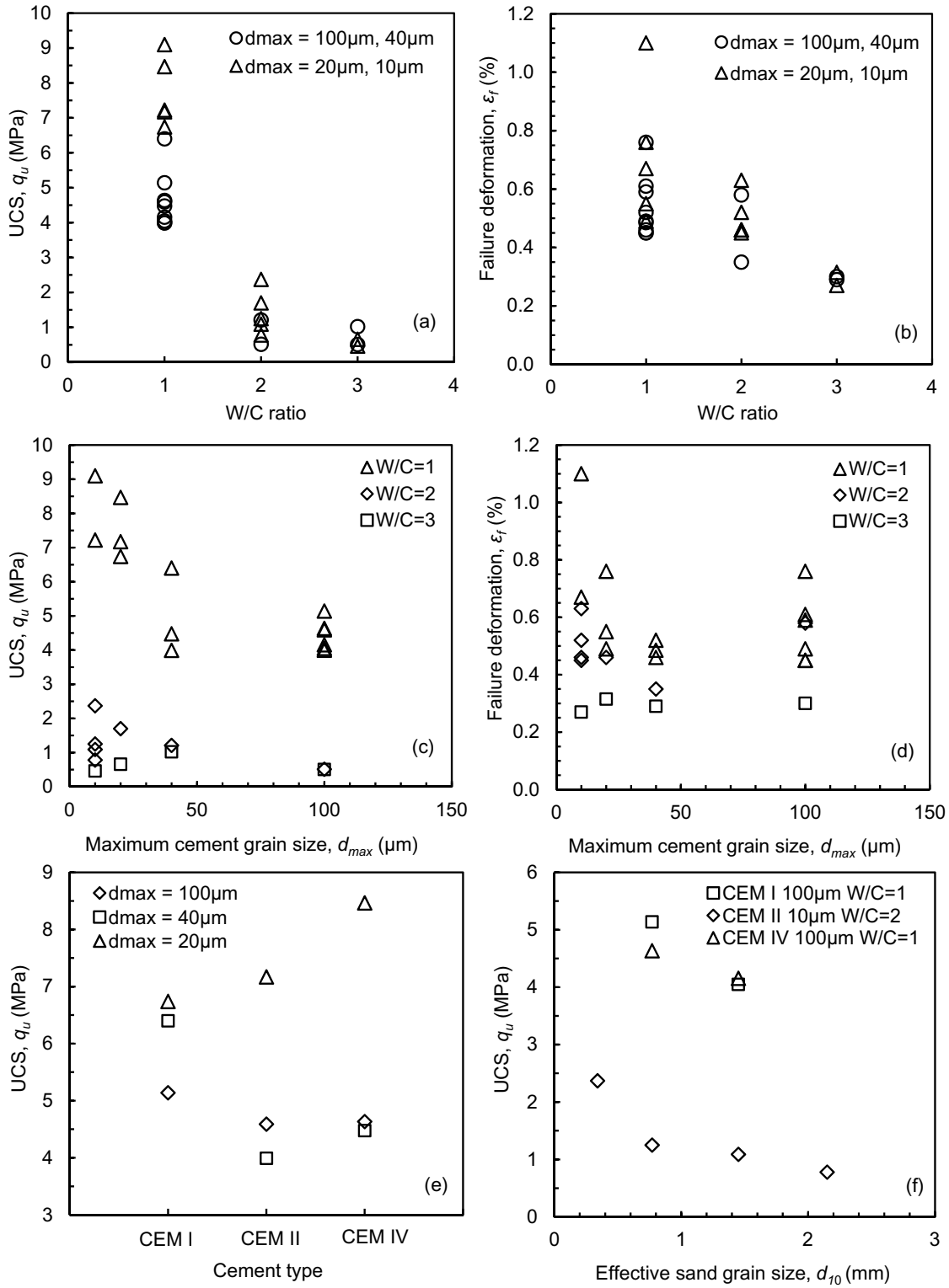

Fig. 3 Effect of grout composition parameters and sand grain size on the unconfined compression strength and failure deformation of grouted sands

strength of grouted sand has also been confirmed by other researchers [e.g., 2, 8, 13, 15, 16, 42, 46, 47] and is attributed to increasing specific surface and number of grain-to-grain contact points per unit volume of sand with decreasing sand grain size resulting in the retention of a greater quantity of grout solids during suspension flow through the soil mass and, hence, in better cementation [2].

UU Triaxial Compression Tests

The results of UU triaxial compression tests can be used to quantify the deformability and shear strength of grouted sands under quick loading conditions and to obtain dependable design parameters for grouting projects. Grouted sand deformability is expressed herein in terms of the initial modulus of elasticity, E_i, (gradient of the tangent to the initial part of the stress–strain curve) and the failure deformation, ε_f, (axial deformation corresponding to the maximum value of deviator stress). The initial modulus of elasticity and the failure deformation of all grouted sands tested exhibit a wide range of values from 3.5 to 44 MPa and from 0.5 to 8.5%, respectively. As typically shown in Fig. 4, linear failure envelopes (K_f-lines) were obtained for all grouted sands subjected to UU testing (total stresses). Accordingly, it can be stated that the shear strength of the grouted sands can be depicted satisfactorily by a Mohr–Coulomb type linear failure criterion and expressed in terms of an angle of internal friction, φ, and a cohesion, c, (total stresses). The same observation has been reported by Pekrioglu-Balkis [27] who conducted the same type of tests on ordinary (CEM I) cement grouted sand after 28 days of curing to obtain baseline values for comparison with the performance of high volume fly ash grouts. The cohesion of the grouted sands ranges between 70 and 1680 kPa, while the angle of internal friction ranges between 40° and 61.5°.

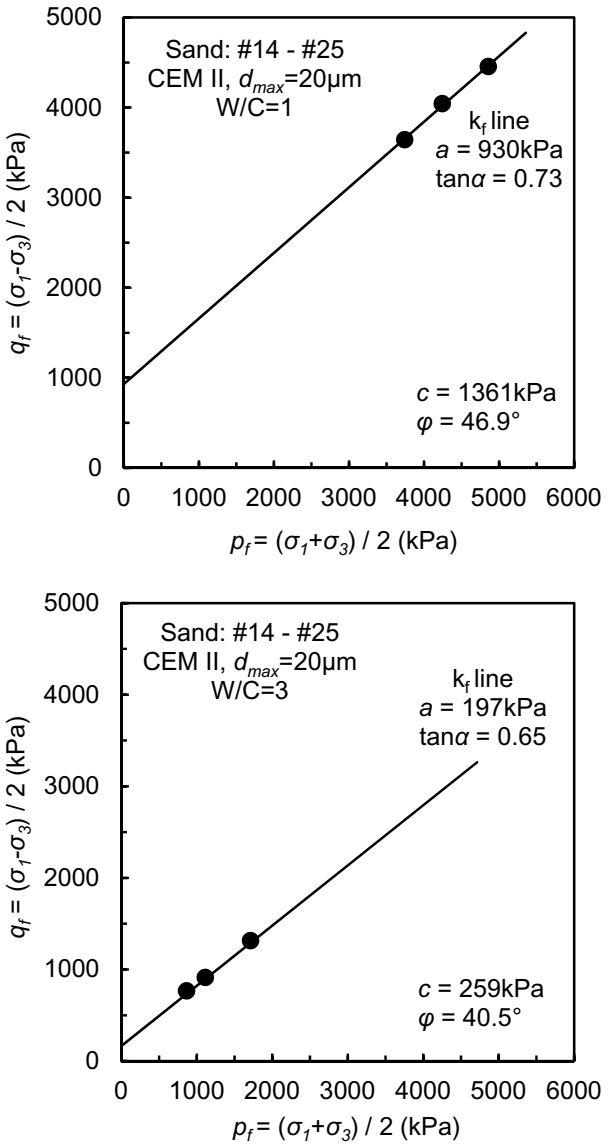

Fig. 4 Typical failure envelopes for grouted sands from UU triaxial compression tests

Effect of Grout Composition

Typical stress–strain curves of sand grouted with suspensions having W/C equal to 1 and 3 together with the stress–strain curves of the clean sand and the neat grout with W/C = 1 are shown in Fig. 5. It can be observed that the sand grouted with the thick suspension (W/C = 1) has a stress–strain curve with a very similar shape to that of the neat grout at the same W/C ratio, whereas the shape of the stress–strain curve of the sand grouted with the thin suspension (W/C = 3) is very similar to that of the clean sand. This observation is typical for all tests conducted and indicates that the stress–strain behavior of the grouted sand depends strongly on the suspension W/C ratio. The initial modulus of elasticity and failure deformation values of the grouted sands are presented in Fig. 6a, b, respectively, in terms of the W/C ratio of the injected suspensions. It is easily observed that a decrease in the W/C ratio from 3 to 1 results in a significant increase in the values of the initial modulus of elasticity and a decrease in the values of the failure deformation. In general, the initial modulus of elasticity of the sands grouted with suspensions having W/C ratio equal to 1, 2 and 3 is in the range of 14–38 MPa, 4.5–12.5 MPa and 3.5–8.5 MPa, respectively, while the failure deformation ranges from 0.5 to 1.4%, from 0.9 to 6.4% and from 2.5 to 8.5%, respectively. The effect of W/C ratio on the shear strength parameters of the grouted sands is presented in Fig. 6c, d. It is apparent that the decrease in W/C ratio increases considerably the cohesion and, to a lesser extent, the angle of internal friction. In particular, sands grouted with suspensions having

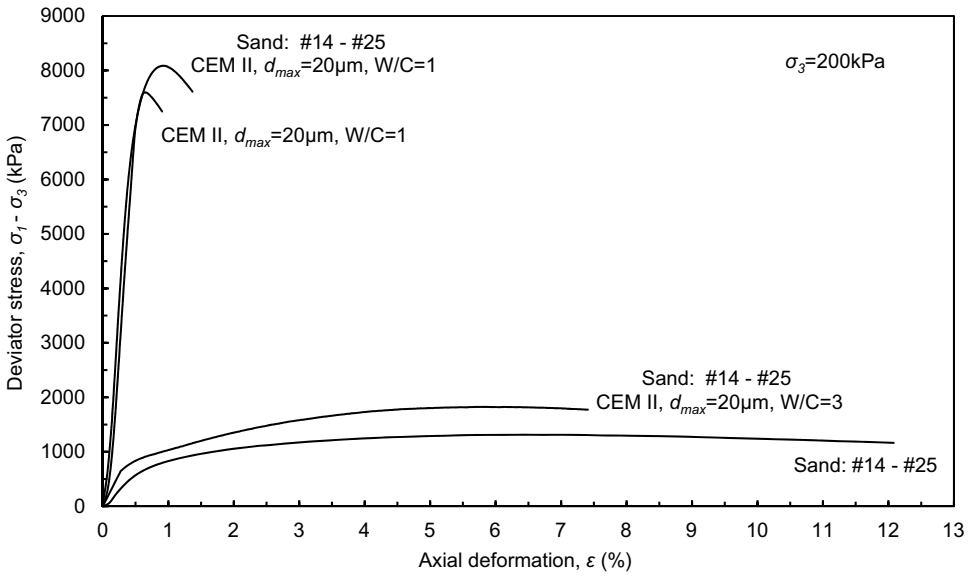

Fig. 5 Stress–strain curves of clean sand, neat cement grout and grouted sand from UU triaxial compression tests

W/C ratios equal to 1, 2 and 3 obtain cohesion values ranging from 630 to 1680 kPa, from 290 to 530 kPa and from 70 to 260 kPa, respectively. It is estimated that thick suspensions (W/C = 1) yield average cohesion values 3 and 7 times higher than those of thinner suspensions (W/C = 2 and 3, respectively). The angle of internal friction values of sands grouted with W/C ratios equal to 1, 2 and 3 range from 43° to 61.5°, from 40° to 45.5° and from 40.5° to 44.5°, respectively.

The effect of cement gradation on the deformability and shear strength parameters of the grouted sands is shown in Fig. 7 as a function of suspension W/C ratio. The initial modulus of elasticity values (Fig. 7a) are not influenced by cement gradation when grouting with W/C ratios equal to 2 and 3, as they range from 3.5 to 11 MPa irrespective of cement grain size. For W/C ratio equal to 1, the E_i values obtained when grouting with pulverized cements (d_{max} equal to 10, 20 and 40 μm) range from 14 to 27 MPa and overlap the values obtained for ordinary cement (d_{max} = 100 μm) which range from 17 to 20 MPa. The failure deformation values (Fig. 7b) increase with decreasing cement grain size for suspensions with W/C ratios equal to 2 and 3, but remain practically constant (0.7% to 1.3%) when using suspensions with W/C ratio equal to 1. In comparison, failure deformations range between 0.4 and 0.9% for neat cement specimens obtained from suspensions having a W/C = 1 regardless of maximum cement grain size. The failure deformation of sands grouted with suspensions having a d_{max} equal to 10, 20, 40 and 100 μm and W/C = 2 ranges from 4 to 5.7%, from 3.3 to 5%, from 3 to 4.7% and from 3.2 to 5%, respectively, whereas it ranges from 6.4 to 8.6%, from 4.5 to 7%, from 2.9 to 5.2% and from 2.5 to 6.1%, respectively, for W/C = 3. As shown in Fig. 7c, the cohesion values of sands grouted with thick suspensions (W/C = 1) and microfine cements (d_{max} = 10 μm and 20 μm) range from 1361 to 1570 kPa and are larger than those obtained for sands grouted with coarser cements (d_{max} = 40 μm and 100 μm) which range from 627 to 841 kPa. On the other hand, grouting with thinner suspensions (W/C = 2 or 3) leads to cohesion values ranging from 70 to 525 kPa regardless of cement grain size. The angle of internal friction of the grouted sands (Fig. 7d) is not consistently affected by cement grain size for any of the W/C ratios used. The UU triaxial compression test results on neat cement grouts presented in Table 2, indicate that the pulverized (d_{max} equal to 10, 20 and 40 μm) CEM II cement suspensions with W/C = 1 exhibit comparable values of deformability and shear strength parameters and, at the same time, higher initial moduli of elasticity, lower failure deformations, higher cohesion values and higher internal friction angles than the equivalent ordinary cement suspension (d_{max} = 100 μm). A comparison of the information presented in Table 2 (neat grout) with the results presented in Fig. 7 (grouted sands) allows the observation that the behavior of cement suspensions is in partial, qualitative and quantitative, agreement with that of the grouted sands indicating that the mechanisms involved in the development of grouted sand properties are complex and do not depend solely on suspension characteristics.

Presented in Table 4 are the deformability and shear strength parameter values of 14–25 sand grouted with suspensions of all three types of microfine cements (d_{max} = 20 μm and 10 μm) having W/C = 1, which allow for an evaluation of the effect of cement type to be made. It is observed that sands grouted with CEM I and CEM IV cement suspensions have similar initial modulus of elasticity values (30–36 MPa) which are higher than those of the sand grouted with CEM II cement suspensions (14–26 MPa). The corresponding neat cement grouts prepared with the three

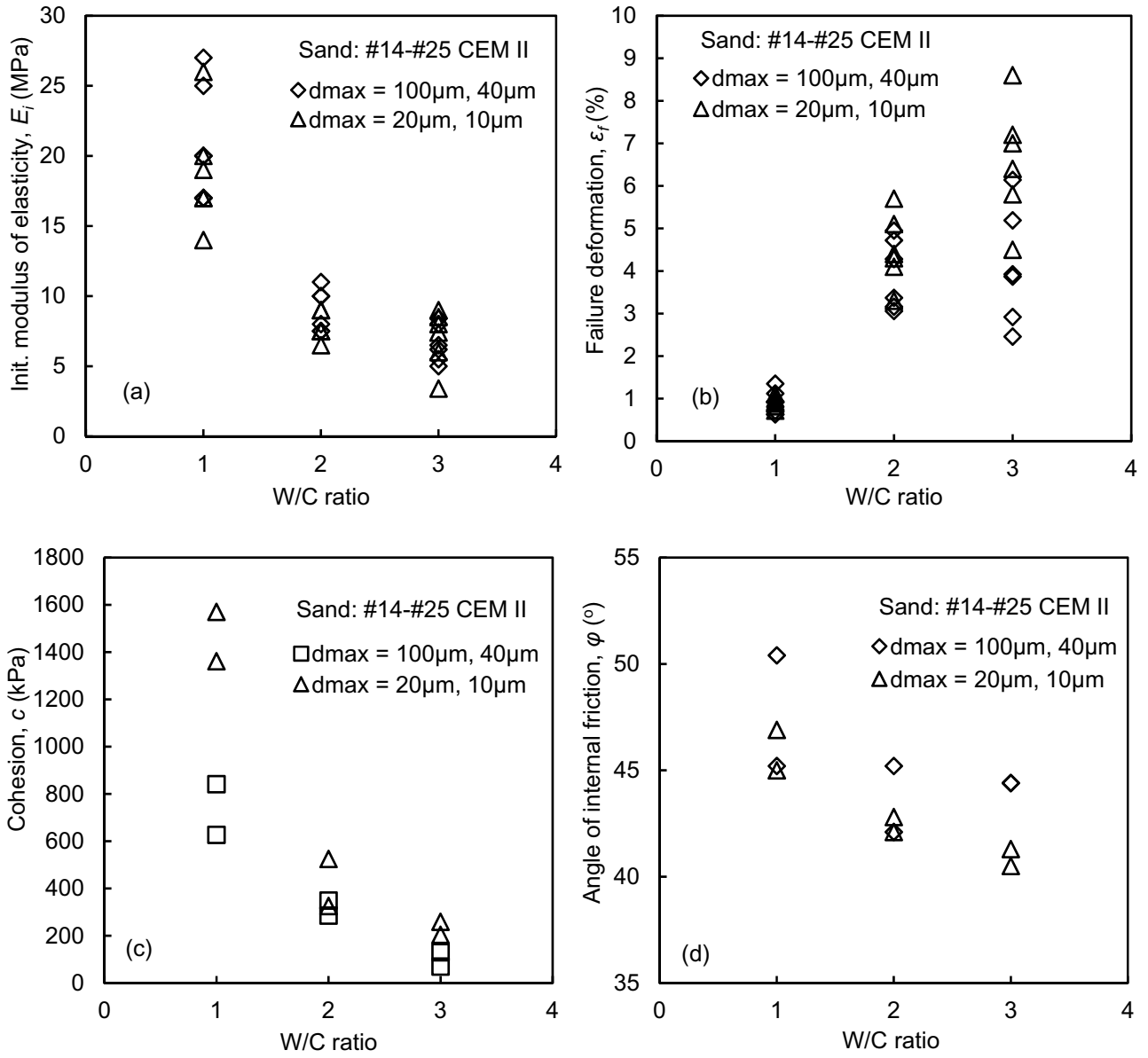

Fig. 6 Effect of W/C ratio on the deformability and shear strength parameters of grouted sands from UU triaxial compression tests

cement types have E_i values ranging from 18 to 29 MPa (Table 2). These values are lower than the E_i values of CEM I and CEM IV cement grouted sands and generally higher than those of CEM II cement grouted sands. Although the failure deformation values of grouted sands are low and generally do not exceed 1.1% (Table 4), the sands grouted with CEM I cement suspensions have slightly lower values (0.6–0.8%) compared to those of sands grouted with CEM II and CEM IV cement suspensions (0.7–1.1%). As shown in Table 2, the failure deformation values of the same microfine cement grouts range from 0.4 to 1.2%, for all cement types tested, and are in good agreement with the failure deformation values of the grouted sands. The available data for the shear strength parameters of the grouted sands and the corresponding neat grouts presented in Tables 2 and 4, respectively, indicate that the CEM IV cement with $d_{max} = 20$ μm presents the best overall performance, the CEM I cement with $d_{max} = 20$ μm presents maximum values for the angle of internal friction for both the grout and the grouted sand and the CEM II cements with d_{max} equal to 20 μm and 10 μm present very high cohesion values for the grouted sand. The cohesion and angle of internal friction values of the grouted sands range from 712 to 1630 kPa and from 45° to 62°, respectively, and are in good agreement with the cohesion and internal friction angle values of the neat grouts which range, respectively, from 560 to 1700 kPa and from 53° to

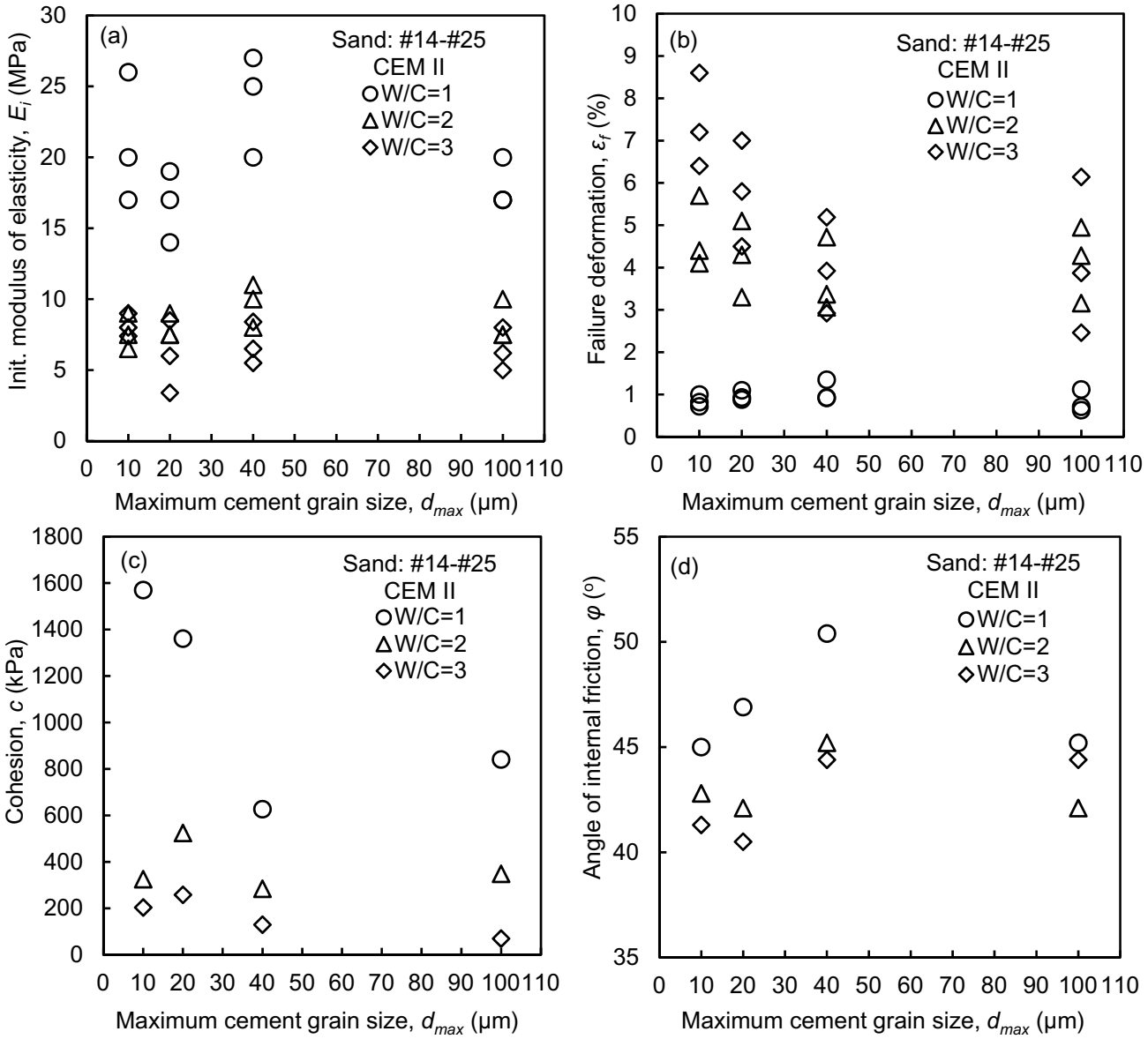

Fig. 7 Effect of cement gradation on the deformability and shear strength parameters of grouted sands from UU triaxial compression tests

61°. It is evident that, regardless of cement type, the shear strength of sands grouted with cement suspensions having W/C = 1 is affected so drastically by the presence of the cement in their voids that, as also shown in Fig. 5, their behavior is similar to that of the neat cement grouts having the same W/C ratio.

Effect of Sand Characteristics

The investigation of the mechanical behavior of grouted sands by UU triaxial compression testing was based mainly on 14–25 sand grouted in dry and dense condition. For reasons of completeness, the effect of sand grain size and initial physical condition (density and saturation) on the mechanical behavior of the grouted sands was also evaluated. Consequently, UU triaxial compression tests were performed on grouted sand specimens obtained by injecting (a) all available sands (5–10, 10–14, 14–25 and 25–50), in dry and dense condition, with the same cement grout (CEM II cement, $d_{\max} = 10$ μm, W/C = 2), and (b) only 14–25 sand at different initial physical conditions (dry-dense, dry-loose, saturated-dense and saturated-loose) with the same cement grout (CEM II cement, $d_{\max} = 10$ μm, W/C = 1). The results obtained, are summarized in Tables 5 and 6, respectively.

As shown in Table 5, sand grain size, in the range studied, has an insignificant effect on the deformability and shear strength parameters of the grouted sands, possibly due to the relatively high suspension W/C ratio (W/C = 2) used for

Table 4 Effect of cement type on the deformability and shear strength parameters of grouted sands (Sand: #14–25, W/C = 1) from UU triaxial compression tests

Cement	Confining pressure σ_3 (kPa)	Initial modulus of elasticity E_i (MPa)	Failure deformation ε_f (%)	Shear strength parameters	
				c (kPa)	φ (°)
CEM I d_{max} = 20 μm	100	30	0.56	712	61.6
	200	34	0.75		
	400	36	0.80		
CEM II d_{max} = 20 μm	100	14	0.88	1361	46.9
	200	17	0.93		
	400	19	1.10		
CEM IV d_{max} = 20 μm	100	36	0.81	1630	59.3
	200	32	1.10		
	400	34	1.00		
CEM II d_{max} = 10 μm	100	17	1.00	1570	45
	200	20	0.72		
	400	26	0.82		
CEM IV d_{max} = 10 μm	100	33	0.90	1143	45.2
	200	31	0.90		
	400	33	1.10		

Table 5 Effect of sand grain size on the deformability and shear strength parameters of grouted sands (CEM II, d_{max} = 10 μm, W/C = 2) from UU triaxial compression tests

Sand	Confining pressure σ_3 (kPa)	Initial modulus of elasticity E_i (MPa)	Failure deformation ε_f (%)	Shear strength parameters	
				c (kPa)	φ (°)
5–10 d_{10} = 2.15 mm	100	4.5	4.5	332	40.0
	200	7	5		
	400	9	6.3		
10–14 d_{10} = 1.45 mm	100	7.2	4.1	326	41.5
	200	9	4.6		
	400	12.5	6.4		
14–25 d_{10} = 0.77 mm	100	6.5	4.1	326	43.0
	200	7.5	4.4		
	400	9	5.7		
25–50 d_{10} = 0.34 mm	100	6	0.9	343	43.5
	200	9.5	2.1		
	400	12	4.1		

the injections. The observed increase of the angle of internal friction with decreasing effective sand grain size is attributed to the increase of both the specific surface of the sand and the number of grain-to-grain contact points per unit volume as sand fineness increases resulting in stronger cementation [2].

The results presented in Table 6 indicate that the failure deformation of the grouted sands is not affected by relative density but attains, generally, lower values, by 12–50%, when the sand is initially saturated. Although a variation is observed in the initial modulus of elasticity values of the grouted sands, a definite trend can not be established for the four initial condition combinations. Dry sands in loose condition have higher initial modulus of elasticity values, by an average of about 50%, than dry sands in dense condition, but the same is not observed for initially saturated sands. As also shown in Table 6, sand density and initial saturation do not appear to affect significantly or systematically the angle of internal friction of the grouted sands. On the contrary, sands grouted in initially dry or loose condition exhibit higher cohesion values, by 15% and 7%, than sands grouted in initially saturated or dense condition, respectively. The observed higher cohesion values for initially dry grouted sand can possibly be attributed to (a) water entrapment in the voids of saturated sand during grouting [48] leading to incomplete filling of the voids with grout and/or (b) the absorption of a quantity of suspension water from the dry sand grains [49] leading to a decrease of suspension W/C ratio during the injection into initially dry sand. In agreement with the results of the present research, Pekrioglu-Balkis [27] measured higher cohesion value for loose sand (D_r = 30%) compared to dense sand (D_r = 83%), both grouted with ordinary (CEM I) cement suspension of W/C = 1 and cured for 28 days. This behavior can possibly be attributed to the retention of a greater quantity of grout solids in the larger pores of a loose sand resulting in more effective cementation.

Deformability and Shear Strength Improvement

The assessment of the improvement caused by grouting on the deformability and shear strength of sands is quantified in the present study using "improvement ratios", i.e., the ratios of the initial modulus of elasticity, E_i, the failure deformation, ε_f, and the angle of internal friction, φ, of the grouted sands to the initial modulus of elasticity, $E_{i,s}$, the failure deformation, $\varepsilon_{f,s}$, and the angle of internal friction, φ_s, of the clean sands, respectively. The results obtained are presented in Fig. 8 with respect to the suspension W/C ratio, since it is the parameter with the most significant effect on the deformability and shear strength of the grouted sands. As shown in Fig. 8a, the increase of the E_i values of sands grouted with suspensions having W/C = 1 (improvement ratios ranging from 7 to 13) is considerably greater than that obtained by grouting with suspensions having W/C ratio equal to 2 or 3 (improvement ratios ranging from 1.5 to 5.5). A substantial improvement of the modulus of elasticity of the sand at small strain conditions was also observed by Maalej et al. [26] after grouting with microfine cement suspensions. The

Table 6 Effect of sand condition before grouting on its deformability and shear strength parameters after grouting (Sand: #14–25, CEM II, $d_{max} = 10$ μm, W/C = 1)

Relative density D_r (%)	Saturation	Confining pressure σ_3 (kPa)	Initial modulus of elasticity E_i (MPa)	Failure deformation ε_f (%)	Shear strength parameters	
					c (kPa)	φ (°)
98	No	100	17	1	1570	45.0
		200	20	0.7		
		400	26	0.8		
25	No	100	18	1.1	1680	44.5
		200	38	0.6		
		400	44	0.8		
98	Yes	100	26.5	0.5	1364	43.0
		200	24	0.5		
		400	25	0.7		
25	Yes	100	27	0.7	1455	46.0
		200	32	0.7		
		400	20	0.7		

failure deformation ratios shown in Fig. 8b, indicate that (a) the grouted sands attain lower values of failure deformation than clean sands and (b) grouting with thick suspensions (W/C = 1) reduces sand failure deformation by 5–10 times, whereas grouting with thinner suspensions (W/C = 2 and 3) reduces sand failure deformation by 2.5 times at the most. The data presented in Fig. 8c, indicate that (a) grouting with suspensions of W/C ratios equal to 2 and 3 results in ratios ranging from 0.95 to 1.05 which means that the angle of internal friction of the sands is practically not affected by the grouting process, and (b) injections with suspensions having W/C = 1 yield improvement ratios ranging approximately from 1.05 to 1.20 indicating that grouting with thick suspension may yield a noteworthy increase, up to 20%, of the angle of internal friction. However, it must be emphasized that the most important contribution of grouting to shear strength improvement of the sands is the addition of cohesion reaching a value of 1680 kPa, as was pointed out in preceding sections.

Shear Strength Development

The development of shear strength of saturated cohesive soils with axial deformation can be quantified and the effective shear strength parameters can be evaluated as functions of axial deformation [50]. The application of this principle to grouted sands has documented that the cohesion and the angle of internal friction of these materials are also functions of the axial deformation and that the sum of their contribution to shear strength is maximum at failure [22, 51–53]. In view of that, the results of UU triaxial compression tests, in terms of total stresses, are utilized herein to quantify the shear strength development of cement grouted sands during loading and up to failure and to compare with that of neat cement grouts and clean sands. The methodology for the quantification of shear strength development was applied (a) by determining, for each test series, the deviator stresses at axial deformations corresponding to specific percentages of failure deformation, (b) by plotting the resulting p-q envelopes (K-lines) for each percentage of failure deformation, and (c) by determining the values of the activated shear strength parameters for all percentages of failure deformation. The concept of percentage of failure deformation ensures that all specimens of the same test series are in an equivalent state of strength development regardless of the confining pressure used for each test.

Presented in Fig. 9 are typical results regarding the variation of the activated cohesion, c_a, and angle of internal friction, φ_a, of grouted sands with increasing axial deformation. The values of activated shear strength parameters and axial deformation are normalized in terms of the failure values of cohesion, c, angle of internal friction, φ, and axial deformation, ε_f, respectively. It can be observed that cohesion development of the grouted sands depends on the W/C ratio of the suspension. More specifically, the cohesion of sands grouted with thick suspensions (W/C = 1) increases gradually until an axial deformation corresponding, approximately, to 70% of the failure deformation (Fig. 9a). At this point, the cohesion reaches a value approximately equal to that obtained at failure and remains nearly constant thereafter. In sands grouted with thin suspensions (W/C ratio equal to 2 or 3), the cohesion exhibits a high rate of increase during the initial stages of axial loading, reaches a maximum value (equal to or greater than that obtained at failure) for an axial deformation approximately equal to 10% of the failure deformation and, then, decreases and either remains practically constant or increases slightly until failure (Fig. 9c). On the contrary, the development of the angle of internal friction of grouted

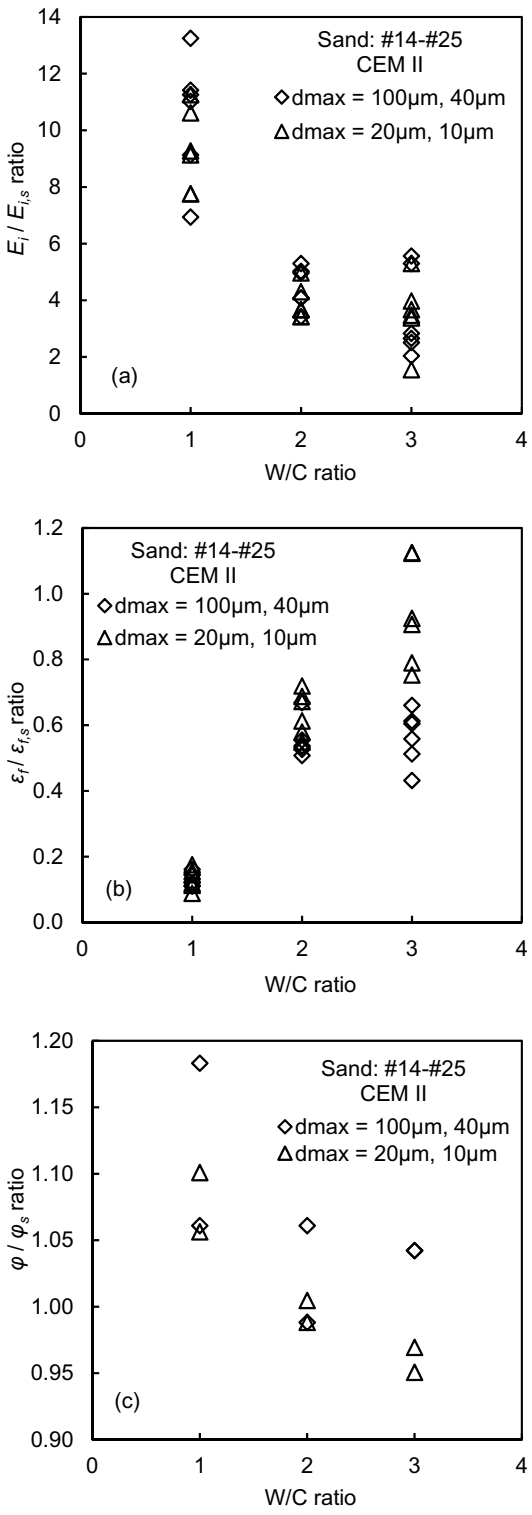

Fig. 8 Variation of the improvement ratios of sand deformability and shear strength parameters as a function of grout W/C ratio

sands does not appear to depend on the use of thick or thin suspension. As shown in Fig. 9b, d, the activated angle of internal friction attains almost its maximum value for an axial deformation ranging between 20 and 30% of the failure deformation and, subsequently, remains practically constant until failure. These observations are in partial agreement with the behavior observed for sands grouted with sodium silicate solutions [51] or microfine cement suspensions [22]. More specifically, it has been reported that the cohesion increases rapidly, reaches a maximum value at low deformation levels, then decreases and maintains a constant value until failure and that the angle of internal friction increases gradually as axial deformation increases and becomes maximum at failure. The observed dissimilarities in behavior can be attributed to the different type or composition of the grouts used in the forementioned research efforts.

The development of the normalized shear strength parameters of grouted sands is compared to that of neat cement suspension and clean sand in Fig. 10. These comparisons are made in terms of the actual values of axial deformation due to the different stress–strain behavior and failure deformation values of the compared materials. The curves presented in Fig. 10a, indicate that the maximum cohesion value of grouted sands develops at relatively low values of axial deformation, ranging between 0.5 and 1%, irrespective of the use of thick or thin suspensions. Cohesion development, in terms of rate and maximum value, of the neat cement suspension with W/C = 1 is very similar to that of the grouted sands. The representative development curves for the angle of internal friction of the grouted sands, shown in Fig. 10b, strongly support the argument that the behavior of sand grouted with a thick suspension is similar to that of neat cement sediments with W/C = 1 and that the behavior of sand grouted with a thin suspension is similar to that of the clean sand, as also stated for the stress – strain curves presented in Fig. 5. These observations can be attributed to the fact that grouting with thick suspensions is most effective, because the sand voids are filled satisfactorily with solidified grout material which also adheres on the surface of the sand grains and provides enhanced cementation to the grouted sand.

Conclusions

Based on the results obtained and the observations made during this experimental investigation and within the limitations of the range of parameters investigated, the following conclusions may be advanced:

1. The suspension W/C ratio has the strongest effect on the behavior and performance of microfine cement grouted sands compared to the effect of the other factors investigated in the present research effort. The stress–strain–strength behavior of sands grouted with thick suspensions (W/C = 1) is similar to that of neat

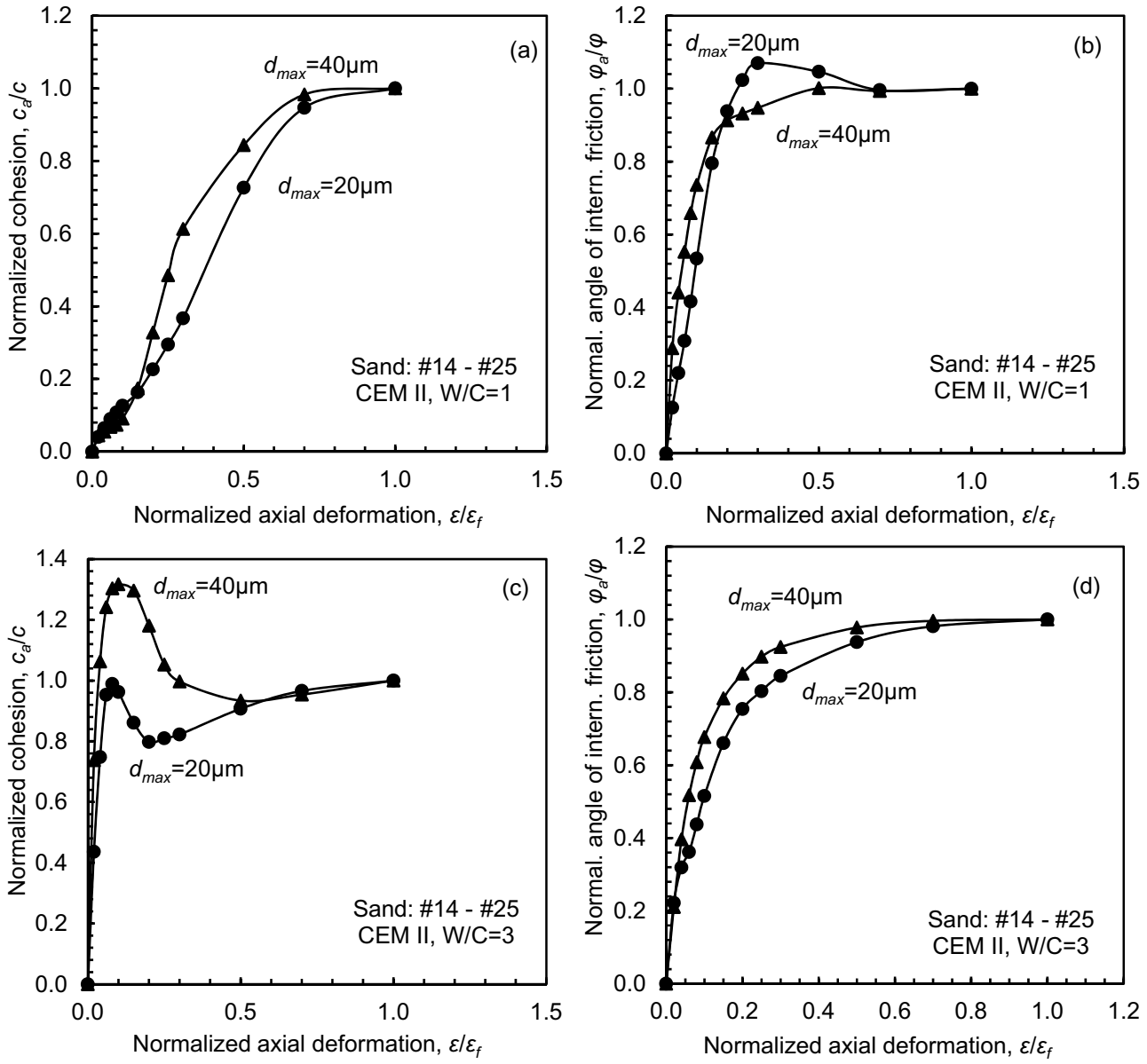

Fig. 9 Variation of the normalized values of the shear strength parameters of grouted sands as a function of normalized axial strain

cement suspension sediments with the same W/C ratio whereas the behavior of sands grouted with thin suspensions (W/C = 3) is similar to that of the clean sands.

2. A Mohr–Coulomb type linear failure criterion describes satisfactorily the shear strength behavior of cement grouted sands, in total stress terms, as obtained by UU triaxial compression tests.
3. The initial modulus of elasticity of the grouted sands ranges from 3.5 to 44 MPa, increases with decreasing suspension W/C ratio and decreases when CEM II cement suspensions are used. The failure deformation of the grouted sands ranges from 0.5 to 8.5%, decreases with decreasing suspension W/C ratio, when CEM I cement suspensions are used and when the sands are initially saturated, and is not affected by sand density. The effect of cement fineness on the deformability parameters of the grouted sands is controlled by the suspension W/C ratio.
4. Grouting with cement suspensions having W/C = 1 adds cohesion to the sand with a value of up to 1.7 MPa, increases by 6–14 times the initial modulus of elasticity, reduces by 5–10 times the failure deformation and may increase up to 20% the angle of internal friction of the sands. The improvement in sand deformability and shear strength due to grouting with suspensions having W/C equal to 2 and 3 is substantially lower, as the added

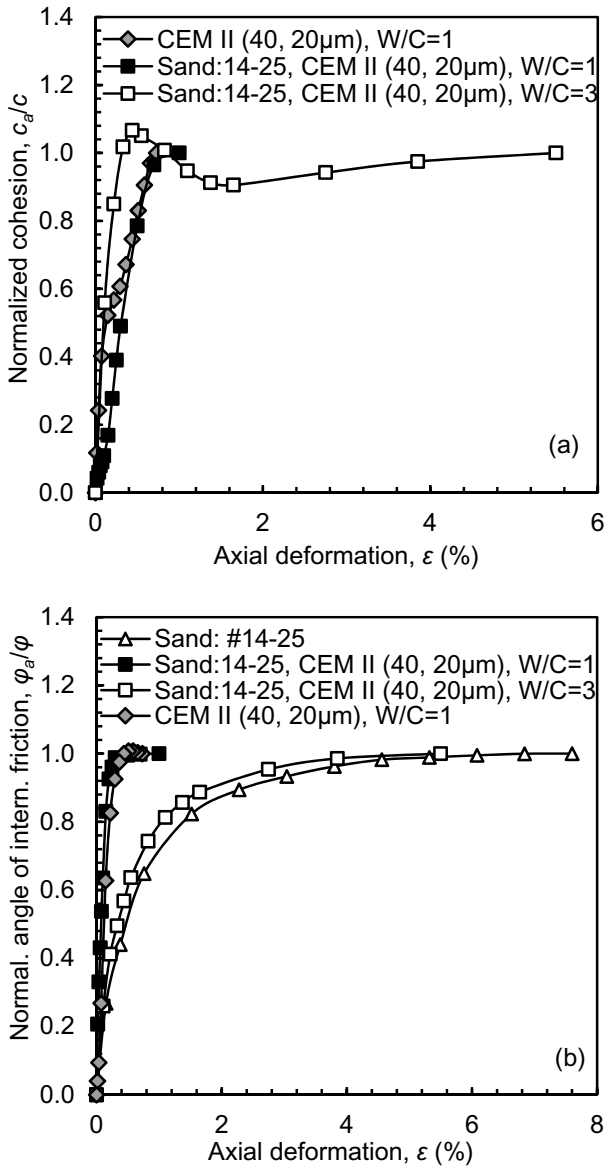

Fig. 10 Comparison of the development rates of the shear strength parameters of grouted sands with those of cement grouts and clean sand

cohesion to the sand reaches 0.53 MPa, the increase of the initial modulus of elasticity ranges from 1.5 to 5.5 times, the reduction of the failure deformation does not exceed 2.5 times and the angle of internal friction of the sands is practically not affected by the grouting process.

5. The cohesion of grouted sands increases with decreasing suspension W/C ratio, when microfine cement suspensions having W/C = 1 are used and when the sands are grouted in initially dry or loose condition. The angle of internal friction of the grouted sands increases to some extent with decreasing suspension W/C ratio and sand grain size and is not consistently or significantly affected by cement fineness and sand density or initial saturation.
6. The development of cohesion and angle of internal friction with increasing axial deformation of microfine cement grouted sands is independent of the use of thick or thin suspensions for grouting. The maximum cohesion value of grouted sands develops at relatively low values of axial deformation, ranging between 0.5 and 1%. The activated angle of internal friction of the grouted sands approaches its maximum value for an axial deformation ranging between 20 and 30% of the failure deformation and, subsequently, remains constant until failure.
7. The unconfined compression strength of the grouted sands attains values up to about 9 MPa, increases with decreasing grout W/C ratio, cement grain size (especially for grouts with W/C = 1) and sand grain size, and is not consistently affected by cement type.

Acknowledgements The research effort reported herein is part of the research project PENED-03ED527, which was co-financed by the European Union—European Social Fund (75%) and the Greek Ministry of Development—General Secretariat for Research and Technology (25%). TITAN Cement Company S.A. contributed chemical analyses, pulverization and grain size analyses of the cements.

Author contributions Conceptualization: INM, DKA; methodology: INM, DKA; formal analysis and investigation: IAP; writing—original draft preparation: IAP, INM; writing—review and editing: INM, DKA; funding acquisition: INM, DKA; resources: INM, DKA; supervision: INM, DKA.

Funding This work was co-funded by the European Union—European Social Fund (75%) and the Greek Ministry of Development—General Secretariat for Research and Technology (25%) (Research project PENED-03ED527).

Availability of data and material All necessary data are provided in the manuscript.

Compliance with ethical standards

Conflict of interest None for any of the authors.

References

1. Henn RW, Soule NC (2010) Ultrafine cement in pressure grouting. ASCE Press, Reston
2. Zebovitz S, Krizek RJ, Atmatzidis DK (1989) Injection of fine sands with very fine cement grout. J Geotech Eng 115:1717–1733. https://doi.org/10.1061/(ASCE)0733-9410(1989)115:12(1717)
3. De Paoli B, Bosco B, Granata R, Bruce D (1992) Fundamental observations on cement based grouts (2): microfine cements and the Cemill^{R} process. In: Proceedings of the Conference on Grouting, Soil Improvement and Geosynthetics, Borden RH, Holtz RD, Juran I (eds), New Orleans, ASCE GSP 30, vol 1, pp 486–499

4. Schwarz LG, Krizek RJ (1994) Effect of preparation technique on permeability and strength of cement-grouted sand. Geotech Test J 17:434–443. https://doi.org/10.1520/GTJ10304J
5. Sano M, Shimoda M, Matsuo O, Koseki J (1996) Microfine cement grouting as a countermeasure against liquefaction. In: Proceedings of the Conference on Grouting and Deep Mixing, Yonekura R, Terashi M, Shibazaki M (eds), vol 1, pp 65–70
6. Santagata MC, Collepardi M (1998) Selection of cement-based grouts for soil treatment. In: Proceedings of the Geo-Congress '98, Johnsen L, Berry D (eds), Boston, ASCE GSP 80, pp 177–195
7. Perret S, Khayat KH, Ballivy G (2000) The effect of degree of saturation of sand on groutability—experimental simulation. Grnd Improv 4:13–22. https://doi.org/10.1680/grim.2000.4.1.13
8. Dano C, Hicher P-Y, Tailliez S (2004) Engineering properties of grouted sands. J Geotech Geoenv Eng 130:328–338. https://doi.org/10.1061/(ASCE)1090-0241(2004)130:3(328)
9. Schwarz LG, Chirumalla M (2007) Effect of injection pressure on permeability and strength of microfine cement grouted sand. In: Proceedings of Geo-Denver 2007—Grouting for Ground Improvement: Innovative Concepts and Applications, Denver, ASCE GSP 168. https://doi.org/10.1061/40912(231)2
10. Mollamahmutoglu M, Yilmaz Y (2011) Engineering properties of medium-to-fine sands injected with microfine cement grout. Mar Georesour Geotechnol 29:95–109. https://doi.org/10.1080/1064119X.2010.517715
11. Mollamahmutoğlu M, Avci E (2015) Ultrafine Portland cement grouting performance with or without additives. KSCE J Civ Eng 19:2041–2050. https://doi.org/10.1007/s12205-014-1445-7
12. Bryson LS, Ortiz R (2016) Mechanical behavior of ultrafine cement—grouted sands under unsaturated conditions. In: Proceedings of Geo-Chicago 2016: Sustainable Geoenvironmental Systems, ASCE GSP 271, pp 816–826. https://doi.org/10.1061/9780784480144.081
13. Avci E, Mollamahmutoğlu M (2016) UCS properties of superfine cement–grouted sand. J Mater Civ Eng 28(12):06016015. https://doi.org/10.1061/(ASCE)MT.1943-5533.0001659
14. El Mohtar CS, Miller AK, Jaffal HA (2017) Introducing a new method for measuring internal stability of microfine cement grouts. In: Proceedings of Grouting 2017: Grouting, Drilling, and Verification, Honolulu, Hawaii, ASCE GSP 288, pp 152–162. https://doi.org/10.1061/9780784480793.015
15. Lee C, Nam H, Lee W, Choo H, Ku T (2019) Estimating UCS of cement-grouted sand using characteristics of sand and UCS of pure grout. Geomech Eng 19(4):343–352. https://doi.org/10.12989/gae.2019.19.4.343
16. Yoon B, Lee W, Lee C, Choo H (2020) Time-dependent variations of compressive strength and small-strain stiffness of sands grouted with microfine cement. J Geotech Geoenviron Eng 146(4):06020001. https://doi.org/10.1061/(ASCE)GT.1943-5606.0002207
17. Krizek RJ, Liao HJ, Borden RH (1992) Mechanical properties of microfine cement/sodium silicate grouted sand. In: Proceedings of the Conference on Grouting, Soil Improvement and Geosynthetics, Borden RH, Holtz RD, Juran I (eds), New Orleans, ASCE GSP 30, vol 1, pp 688–699
18. Clarke WJ, Boyd MD, Helal M (1993) Ultrafine cement tests and drilling Warm Springs dam. In: Proceedings of Specialty Conference on Geotechnical Practice in Dam Rehabilitation, Anderson LR (ed), Raleigh, North Carolina, ASCE GSP 35, pp 718–732
19. Dano C, Hicher P-Y (2003) Behavior of uncemented sands and grouted sands before peak strength. Soils Found 43(4):13–19. https://doi.org/10.3208/sandf.43.4_13
20. Maalej Y, Dormieux L, Canou J, Dupla J-C (2007) Strength of a granular medium reinforced by cement grouting. Comptes Rendus Mécanique 335(2):87–92. https://doi.org/10.1016/j.crme.2006.12.003
21. Kainrath A, Adam D (2015) Influences on the mechanical behavior of grouted soil. In: Proceedings of the XVI ECSMGE, Geotechnical Engineering for Infrastructure and Development, ICE Publishing, pp 2951–2956. https://doi.org/10.1680/ecsmge.60678
22. Krizek RJ, Atmatzidis DK, Wu ZH (1986) Behavior of grouted Erksak sand. Northwestern University, Department of Civil Engineering, Evanston
23. Naeini SA, Ziaie–Moayed R (2003) Undrained shear strength and liquefaction potential of loose silty sand treated with microfine cement. In: Proceedings of the 13th European Conference on Soil Mechanics and Geotechnical Engineering, Prague, vol 1, pp 849–854
24. Jafarpour P, Moayed RZ, Kordnaeij A (2020) Yield stress for zeolite-cement grouted sand. Constr Bldg Mater 247:118639. https://doi.org/10.1016/j.conbuildmat.2020.118639
25. Jafarpour P, Moayed RZ, Kordnaeij A (2020) Behavior of zeolite-cement grouted sand under triaxial compression test. J Rock Mech Geotech Eng 12(1):149–159. https://doi.org/10.1016/j.jrmge.2019.06.010
26. Maalej Y, Dupla J-C, Canou J, Maalej Y, Dormieux L (2007) Caractéristiques de déformabilité d'un sable injecté par un coulis de micro ciment. In: Proceedings of the 14th European Conference on Soil Mechanics and Geotechnical Engineering, Madrid, vol 3, pp 1361–1365
27. Pekrioglu-Balkis A (2020) Properties and performance of a high volume fly ash grout. Mar Georesour Geotechnol 38(1):73–82. https://doi.org/10.1080/1064119X.2018.1552999
28. Yao W, Pang J, Liu Y (2018) An experimental study of Portland cement and superfine cement slurry grouting in loose sand and sandy soil. Infrastructures 3(2):9. https://doi.org/10.3390/infrastructures3020009
29. Markou IN, Christodoulou DN, Papadopoulos BK (2015) Penetrability of microfine cement grouts: experimental investigation and fuzzy regression modeling. Can Geotech J 52:868–882. https://doi.org/10.1139/cgj-2013-0297
30. Markou IN, Christodoulou DN, Petala ES, Atmatzidis DK (2018) Injectability of microfine cement grouts into limestone sands with different gradations: experimental investigation and prediction. Geotech Geol Eng 36:959–981. https://doi.org/10.1007/s10706-017-0368-8
31. Markou IN, Kakavias ChK, Christodoulou DN, Toumpanou I, Atmatzidis DK (2020) Prediction of cement suspension groutability based on sand hydraulic conductivity. Soils Found 60(4):825–839. https://doi.org/10.1016/j.sandf.2020.05.011
32. Pantazopoulos IA, Atmatzidis DK (2012) Dynamic properties of microfine cement grouted sands. Soil Dyn Earthq Eng 42:17–31. https://doi.org/10.1016/j.soildyn.2012.05.017
33. CEN (European Committee for Standardization) (2000) Cement—Part 1: composition, specifications and conformity criteria for common cements. European Standard EN 197-1, Brussels, Belgium
34. CEN (European Committee for Standardization) (2000) Execution of special geotechnical work – Grouting. European Standard EN 12715, Brussels, Belgium
35. Littlejohn GS (1982) Design of cement based grouts. In: Proceedings of the Conference on Grouting in Geotechnical Engineering, Baker WH (ed), New Orleans, ASCE, vol 1, pp 35–48
36. Eriksson M, Friedrich M, Vorschulze C (2003) Variations in the rheology and penetrability of cement-based grouts—an experimental study. Cem Concr Res 34:1111–1119. https://doi.org/10.1016/j.cemconres.2003.11.023
37. Bruce DA, Littlejohn GS, Naudts CA (1997) Grouting materials for ground treatment: a practitioner's guide. In: Proceedings of the Conference on Grouting: Compaction—Remediation—Testing, Vipulanandan C (ed), Logan, ASCE GSP 66, pp 306–334

38. Lombardi G (2003) Grouting of rock masses. In: Proceedings of the 3rd International Conference on Grouting and Ground Treatment, Johnsen FL, Bruce AD, Byle JM (eds), New Orleans, ASCE GSP 120, vol 1, pp 164–197. https://doi.org/10.1061/40663(2003)6
39. Pantazopoulos IA, Markou IN, Christodoulou DN, Droudakis AI, Atmatzidis DK, Antiohos SK, Chaniotakis E (2012) Development of microfine cement grouts by pulverizing ordinary cements. Cem Concr Comp 34:593–603. https://doi.org/10.1016/j.cemconcomp.2012.01.009
40. ASTM (American Society for Testing and Materials) (2009) Standard specification for wire cloth and sieves for testing purposes. Standard E11, ASTM International, West Conshohocken
41. ASTM (American Society for Testing and Materials) (2002) Standard test method for laboratory preparation of chemically grouted soil specimens for obtaining design strength parameters. Standard D4320–02, ASTM International, West Conshohocken
42. Kordnaeij A, Moayed RZ, Soleimani M (2019) Unconfined compressive strength of loose sandy soils grouted with zeolite and cement. Soils Found 59(4):905–919. https://doi.org/10.1016/j.sandf.2019.03.012
43. Li Z, Zhang L, Chu Y, Zhang Q (2020) Research on influence of water-cement ratio on reinforcement effect for permeation grouting in sand layer. Adv Mater Sci Eng 2020:5329627. https://doi.org/10.1155/2020/5329627
44. Shibata H (1996) Study on long-term strength properties of suspension grouts with ultra-fine-grain materials. In: Proceedings of the Conference on Grouting and Deep Mixing, Yonekura R, Terashi M, Shibazaki M (eds), vol 1, pp 71–76
45. Akbulut S, Saglamer A (2002) Estimating the groutability of granular soils: a new approach. Tunn Undergr Sp Technol 17(4):371–380. https://doi.org/10.1016/S0886-7798(02)00040-8
46. Dupla J-C, Canou J, Gouvenot D (2004) An advanced experimental set-up for studying a monodirectional grout injection process. Grnd Improv 8:91–99. https://doi.org/10.1680/grim.2004.8.3.91
47. Schwarz LG, Krizek RJ (2006) Hydrocarbon residuals and containment in microfine cement grouted sand. J Mater Civ Eng 18(2):214–228. https://doi.org/10.1061/(ASCE)0899-1561(2006)18:2(214)
48. O'Connor KM, Krizek RJ, Atmatzidis DK (1978) Microcharacteristics of chemically stabilized granular materials. J Geotech Eng Div 104(7):939–952
49. Perret S, Ballivy G, Khayat K, Mnif T (1997) Injectability of fine sand with cement-based grout. In: Proceedings of the Conference on Grouting: Compaction—Remediation—Testing, Vipulanandan C (ed), Logan, ASCE GSP 66, pp 289–305
50. Schmertmann JH, Osterberg JO (1960) An experimental study of the development of cohesion and friction with axial strain in saturated cohesive soils. In: Proceedings of Research Conference on Shear Strength of Cohesive Soils, Boulder, ASCE, pp 643–694
51. Krizek RJ, Benltayf MA, Atmatzidis DK (1982) Effective stress – strain – strength behavior of silicate-grouted sand. In: Proceedings of the Conference on Grouting in Geotechnical Engineering, Baker WH (ed), New Orleans, ASCE, vol 1, pp 482–497
52. Markou IN, Atmatzidis DK (2003) Mechanical behavior of a pulverized fly ash grouted sand. Geotech Test J 26(4):450–460. https://doi.org/10.1520/GTJ11252J
53. Markou IN, Droudakis AI (2013) Shear strength of microfine cement grouted sands. Grnd Improv 166(3):177–186. https://doi.org/10.1680/grim.12.00016